Visualization of Tensile Stress Induced Material Response at a Crack Tip in Polymers under Critical Load by NMR Imaging

P. Adriaensens, L. Storme, R. Carleer, D. Vanderzande, and J. Gelan*

Limburg University, Instituut voor Materiaalonderzoek (IMO), Department SBG, Universitaire Campus, Gebouw D, B-3590 Diepenbeek, Belgium

V. M. Litvinov*,† and R. Marissen†,‡

DSM Research, P.O. Box 18, 6160 MD Geleen, The Netherlands, and Delft University of Technology, Faculty of Mechanical Engineering, Mekelweg 2, 2628 CD Delft, The Netherlands

Received October 5, 1999

ABSTRACT: NMR imaging is applied to study the crack growth resistance of polymers, being an important toughness parameter of which the understanding is still incomplete. A dedicated stretching device was developed to keep notched materials under load during the NMR measurements allowing to visualize the near crack tip damage behavior in polymers. Two polymers were investigated: ABS, a blend of poly(styrene-*co*-acrylonitrile) with 28 wt % polybutadiene, and a block copolymer poly(butylene terephthalate)/poly(tetramethylene oxide) (PBT/PTMO). MRI investigations were performed on loaded specimens with a crack grown under critical conditions as well as on unloaded specimens. Numerous damage bands appear in the images of strained ABS which converge toward the crack tip and remain present upon unloading. Image contrast is demonstrated to arise from a reduced material density in these damage bands. The material density near the crack tip is reduced to about one-fourth of the normal density. Obviously severe crazing and rubber particle cavitation occurs at the crack tip. For the PBT/PTMO block copolymer a more continuous distribution of stress induced material response is observed that disappears almost completely upon unloading. Here image contrast mainly arises from a reduction of chain mobility in soft domains due to stress induced chain orientation.

Introduction

To improve the fracture resistance of polymers, a better understanding of the fracture processes is important. A large amount has been learned in the past 20 years about the processes of crack propagation in glassy polymers[1−7] and rubber-toughened plastics.[8−10] Despite these useful studies, the understanding of crack growth resistance is incomplete mainly due to the small scale on which the near crack tip fracture processes occur and because crack propagation occurs under critical conditions of mechanical load. Moreover, most of the relevant fracture processes occur in the bulk of the material, shielded by surrounding material, limiting the usefulness of conventional microscopes. Consequently, studies on the material morphology in the near crack tip region are rare and most often limited to the fracture surface, which is investigated post-mortem.[11,12] For example, Riemslag[13,14] studied a craze zone at the crack tip in PE by SEM. Therefore, slices perpendicular to the crack tip were cut out of a stress relaxed plate, and SEM pictures were recorded after reloading the slices. Although illustrative, this method is elaborate and still suspect to artifacts, mainly regarding the reloading of the specimen. NMR imaging offers a possibility to overcome this limitation.

NMR imaging (MRI) is a well-established, nondestructive and noninvasive tool[15,16] well-suited to study the microscopic spatial dependency of stress induced material response.[17−19] As opposed to optical and electron microscopy which only allow to study the material surface or require transparent materials, NMR microimaging can be performed slice selective in the bulk of the material. Moreover, material preparation like deuteration for neutron scattering is not required. Several MRI techniques were previously used for characterization of rubbers and semicrystalline and rigid polymers under deformation.[18−24] It was shown that the method provides information on strain distribution, the direction of local strain, molecular order, variation in the local mobility, and inhomogeneous sample heating under dynamic mechanical load.

Although the spatial resolution of MRI, being about 50 μm or less, is rather low as compared to that of TEM and SEM,[15,16,25] the method provides complementary information because of the large variety of molecular dependent contrast parameters, like the spin density (M_0) and the relaxation times T_{1H}, $T_{1\rho H}$, and T_{2H}, that can be implemented.[18,26,27] These parameters can be related to the amount of material/phases per unit volume and molecular mobility. Quantitative spin-density and relaxation time images can be of particular interest for the characterization of a growing crack.

In this paper, NMR imaging of cracked polymeric materials under critical load is reported. To acquire images under load, a dedicated, stress-calibrated stretching device, which fits into the MRI probe head, was developed. Etching of distance markers on the tensile bars further allows the estimation of a stress−strain relation. Two types of materials were studied: ABS, a blend of poly(styrene-*co*-acrylonitrile) (SAN) with 28 wt % PB (polybutadiene), and a block copolymer of poly(butylene terephthalate) (PBT) and poly(tetramethylene oxide) (PTMO). ABS is a tough amorphous engineering thermoplastic, consisting of a SAN copolymer matrix

† DSM Research.
‡ Delft University of Technology.
* To whom correspondence should be addressed.

10.1021/ma991675t CCC: $19.00
Published on Web 06/01/2000

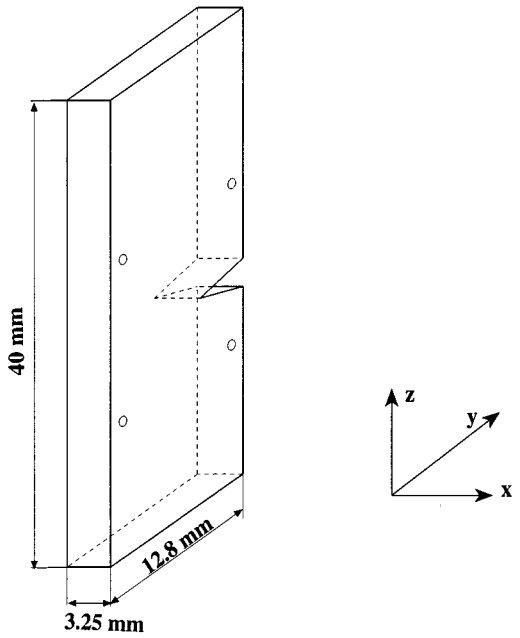

Figure 1. Sample size and its position in the magnet with respect to the B_0 field (*z*-direction). The 4 mm notch and the distance markers are indicated. The strain is parallel to the *z*-direction.

blended with submicron SAN grafted polybutadiene rubber particles. The PBT/PTMO block copolymer belongs to the class of thermoplastic elastomers. Hard PBT blocks and soft PTMO blocks form a co-continuous phase structure.[28] The hard segments crystallize upon cooling from the melt and provide the physical links. These two materials reveal a large difference in the crack growth. While the PBT/PTMO block copolymer shows a more continuous distribution of stress induced material response, ABS clearly shows strongly localized damage bands which are to our knowledge not visualized in this detail so far.

Experimental Section

Materials. Two types of polymer materials were studied: ABS, a blend of poly(styrene-*co*-acrylonitrile) (SAN) with 28 wt % SAN grafted poly(butadiene) (PB), and a block copolymer of poly(butylene terephthalate) (PBT) and poly(tetramethylene oxide) (PTMO). The average block length of the PTMO blocks is 1000 g/mol, and the amount of PTMO is 35 wt %. The molecular weight M_n of the block copolymer is about 25 000 g/mol. The M_w/M_n ratio for PTMO and PBT blocks is about 1.6 and 2, respectively.

All samples for the MRI study have a dimension of 40 × 12.8 × 3.25 mm. The plates were sawn out of an original injection molded plate of 120 × 12.8 × 3.25 mm.

Material Loading. To study the process of crack growth, a cracked specimen under load is required at the condition of a (very slowly) growing crack. To obtain such a condition, a sharp notch of 4 mm in depth was cut in the plates perpendicular to the strain direction *z* (Figure 1). Preliminary tensile strength tests on ABS specimens showed that the notch does not change the yield stress, being around 30 MPa, significantly. The fracture of such small specimens of a tough material occurs by net section yielding. A dedicated stretching device has been developed to measure samples under constant strain (Figure 2). The specimen was fixed in copper top and bottom clamps by two screws on each clamp. The distance between the screws on each clamp is 5 mm. While the glass tube fixes the bottom piece, the top piece can be pulled up by a screw bar resulting in the elongation of the specimen. The stress induced on the plate can roughly be estimated from the torque used to load the screw bar. Distance markers were etched on one side of the plate, about 5 mm above and below the notch. These markers make it possible to measure the average strain as a function of increasing stress.

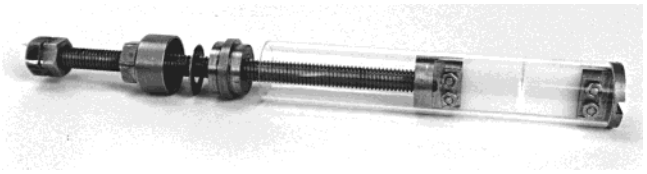

Figure 2. A picture of the stretching device.

The loading of the notched specimen is accomplished outside of the NMR magnet. The specimen was elongated until about 0.6−1 mm crack growth was observed. The load was maintained on the specimen during the NMR imaging investigations. Consequently, the crack tip region could be investigated under critical conditions. Furthermore, additional experiments were performed after unloading the specimen.

Imaging. ^{1}H MRI spin echo images are generated at 9.4 T on an Inova 400 Varian vertical bore spectrometer with a spin-warp pulse sequence in a microimaging probe with a coil of 16 mm in diameter. The sample was positioned such that the static magnetic field B_0 was parallel to the straining direction (Figure 1).

Images of ABS are acquired with an echo time (TE) of 1.51 ms and a repetition delay (TR) of 1 s and have an in-plane pixel resolution of 66 × 66 μm, a field of view (FOV) of 16 × 20 mm, and a slice thickness of 3.25 mm (48 accumulations) or 1.625 mm (48 or 128 accumulations). Images of PBT/PTMO are acquired with TE = 1.05 ms and TR = 1 s and have an in-plane resolution of 100 × 100 μm, a FOV of 16 × 20 mm, a slice thickness of 2 mm, and 100 accumulations. Slice selective images were always taken nicely in the center of the plates (Figure 1) by tuning the offset frequency in the slice direction. Typical gradient strengths used were 30.8, 13.2, and 25.9 G/cm for phase, read, and slice direction, respectively.

The spin density (M_0) and the spin−spin relaxation time (T_2) for different picture elements were determined by analysis of the echo amplitude as a function of TE (13 values between 1.10 and 2.40 ms) with a fixed TR of 1.25 s, using the following relation:

$$\ln M(\mathrm{TE}) = \ln M_0 - \mathrm{TE}/T_2 \qquad (1)$$

All images selectively visualize the rubber phase since transverse magnetization of the rigid matrix decays to zero within 100 μs. The biexponential T_2 relaxation behavior of these materials, due to glassy polymer and rubbery phase, is filtered by the rather long spin echo time (TE).

The spatial dependence of the spin−lattice relaxation time (T_1) and M_0 was determined from a series of images taken as a function of TR (10 values between 0.25 and 4 s) with a fixed TE of 1.10 ms, according to the following relation:[29]

$$M(\mathrm{TR}) = M_0(1 - \mathrm{e}^{-\mathrm{TR}/T_1})\mathrm{e}^{-\mathrm{TE}/T_2} \qquad (2)$$

The reference value represents an average of 10 unaffected locations.

The images used for this quantitative analysis have a slice thickness of 1.625 and 2 mm for ABS and PBT/PTMO, respectively.

Results and Discussion

Figure 3a presents a reference image of a native ABS plate showing the notch and the distance markers etched at about 5 mm on both sides of the notch. Although the determination of the stress−strain relation is not the goal of this study, Figure 4 shows the relation obtained for ABS out of a series of images taken

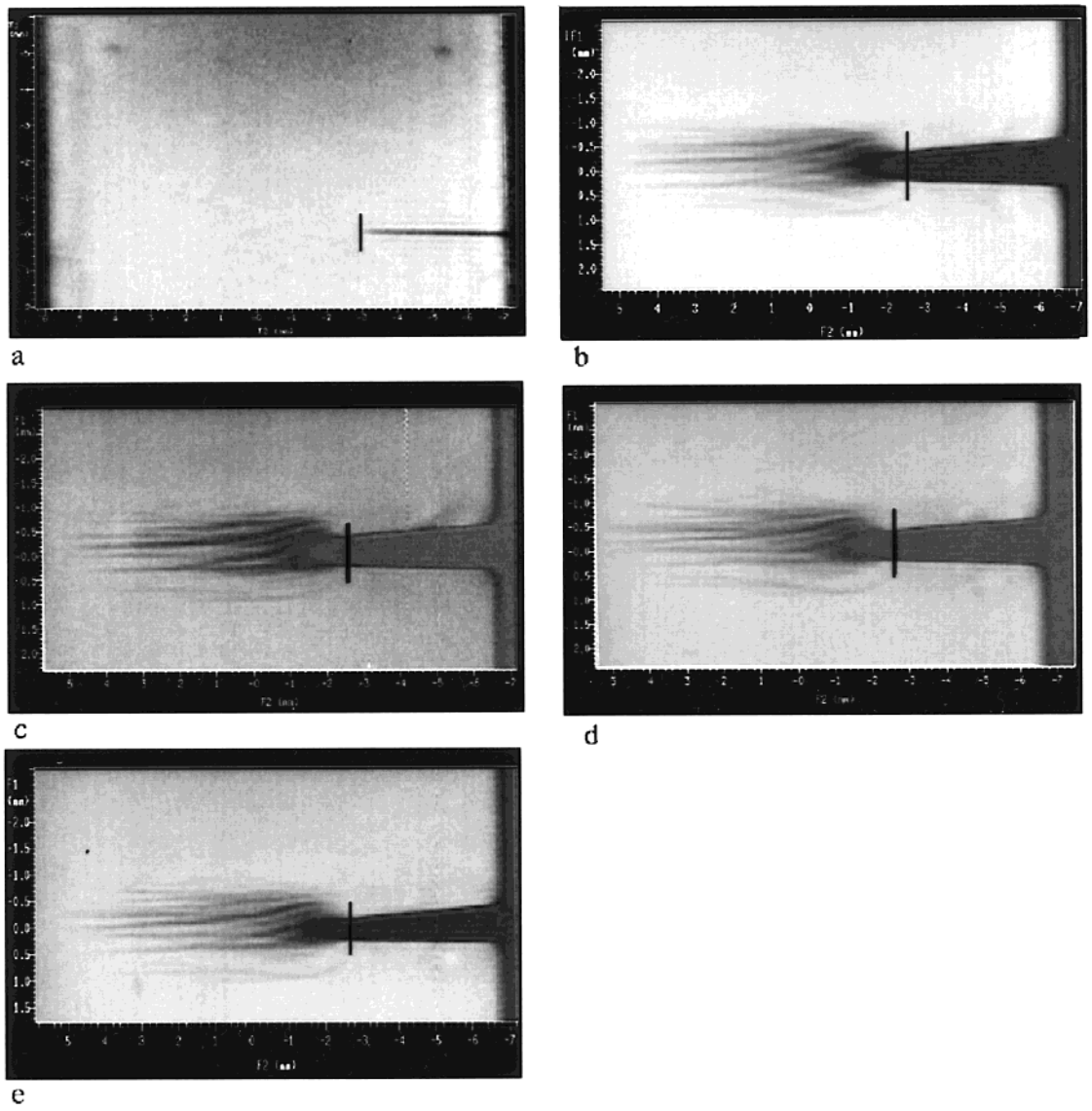

Figure 3. (a) Reference scout image of an ABS plate showing the notch and the distance markers (dark circles), (b) image of a 3.25 mm slice of ABS under critical load, (c) idem but with a slice thickness of 1.625 mm of the outer part of the plate (48 accumulations), (d) idem but with a slice thickness of 1.625 mm of the inner part of the plate (128 accumulations), and (e) idem after unloading (128 accumulations). The depth of the original notch is indicated by a vertical line.

as a function of increasing load. The percentage strain was determined by the relation

$$\epsilon = \frac{l - l_0}{l_0} \times 100$$

in which l_0 is the initial distance between the markers and l the distance after stretching.

Further drawing leads to a break of the material. The material yield stress is overestimated by about 33%, due to friction between the screw bar and the nut during straining. However, this difference is sufficiently small in view of the goal of this study.

Images of an ABS plate under critical load (around 8% elongation) are shown in Figure 3b−d. Tensile stress clearly results in the appearance of numerous damage bands in the material which converge toward the crack tip. Since the transverse magnetization of the rigid glassy matrix decays to zero within 100 μs, the biexponential T_2 relaxation behavior of these materials has been filtered out in our images taken with an echo time of 1.0−1.5 ms. The echo time acts as a highly selective

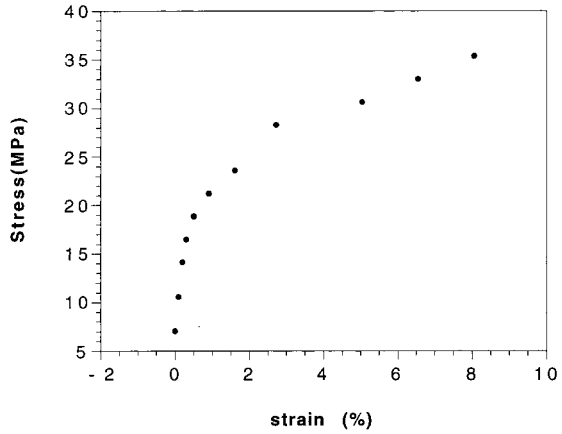

Figure 4. Stress−strain curve measured for ABS with the stretching device; further loading leads to break of the material.

T_2 relaxation time filter resulting in images that show the strain effect only for the rubbery phase of the specimen. Figure 3 illustrates that useful insights in the fracture process of polymer materials can already

Table 1. Spatial Dependence of the Spin Density (M_0) and T_2 and T_1 Relaxation Time for ABS under Critical Load and after Unloading; the Positions Are Indicated in Figure 5[a]

	loaded		unloaded		loaded		unloaded	
fixed spatial position	T_2 (ms)	M_0	T_2 (ms)	M_0	T_1 (s)	M_0	T_1 (s)	M_0
1	1.00	90	0.98	92	0.72	91	0.78	96
2	1.02	75	0.98	84	0.73	76	0.74	86
3	0.91	78	0.90	88	0.77	69	0.75	77
4	0.94	54	0.94	62	0.75	52	0.73	62
5	0.96	35	0.96	42	0.72	31	0.84	43
6	1.06	22	1.06	26	0.71	23	0.74	30
7	0.95	42	0.96	40	0.68	38	0.76	39
8	1.08	28	0.88	52	0.75	34	0.71	46
ref	1.00	100	0.98	100	0.75	100	0.77	100

[a] The averaged 95% confidence limit is 5% for the relaxation times and 2% for the M_0 values.

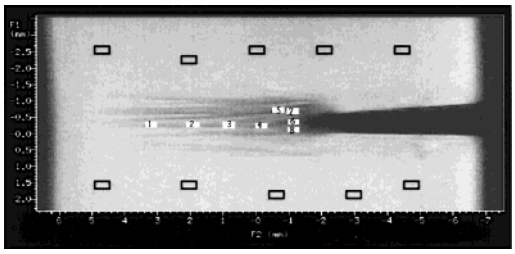

Figure 5. Image of ABS showing the fixed spatial locations where the spin density (M_0) and T_1 and T_2 relaxation times were determined. For values see Table 1. All picture elements are 0.16 × 0.31 mm in dimension. The reference spots (black rectangles) have a similar dimension and are located at least 1.5 mm from the damage bands.

be obtained by analyzing strain induced phenomena in the viscoelastic phase using spin-warp imaging techniques without advanced solid-state imaging methods.[15,30] Reducing the slice thickness (compare partsb and c, d of Figure 3) significantly improves the detection of morphological details in the damage bands and around the crack tip. By comparing parts c and d of Figure 3, it becomes clear that the structure of the damage bands is not completely homogeneous over the thickness of the plate, explaining the influence of slice thickness on image detail. To our knowledge, damage bands in ABS under deformation were not visualized in this detail so far.

Images of the same sample shortly after unloading reveal that the damage bands remain present and are almost unaffected by unloading (Figure 3e). The structure of the damage bands remains, even 24 h after unloading.

To study whether the image appearance of the damage bands is caused by changes in material density and/or strain induced chain orientation (molecular mobility) in the rubbery phase, the spatial dependence of M_0 and of the T_1 and T_2 relaxation times was determined. The relaxation times T_2 and T_1 provide information on slow, long spatial scale and fast, local chain mobility, respectively. The proton spin-density (M_0) is directly related to the density of material. A quantitative, spatial dependent determination of these parameters is extracted out of a series of images taken as a function of TE (T_2 and M_0) and as a function of TR (T_1 and M_0).

Table 1 shows the values of M_0, T_1, and T_2 for several picture elements in the image of ABS under critical load (Figure 5) and after unloading. No significant spatial differences in T_2 and T_1 can be detected in the damage bands neither under load nor after unloading as compared to the reference values in areas that are not affected by strain. This means that the decrease in image intensity in the damage bands cannot be attributed to a strain induced decrease of segmental mobility or strain induced chain orientation in the rubbery phase. This is confirmed by spatial dependent T_2 relaxation measurements on an unloaded sample at different angles with respect to the magnetic field, showing no angular dependency of the localized T_2 values.

On the other hand, a significant reduction of M_0 is observed in the (dark) regions of the damage bands. The material density in the near crack tip region is reduced to about one-fourth of the normal density due to severe rubber particle cavitation. Moreover, the density decrease extends to a "large" distance from the crack tip. Unloading results in a partial recovery in the density of the material in the damage zone although the structure of the damage bands remains unchanged. The fracture resistance of rubber-toughened plastics is now known to be critically dependent upon void formation in the rubber phase.[31,32] In most types of toughened plastics, cavitation of the rubber particles ahead of a crack tip is followed by shear yielding in the intervening matrix to form dilution bands, thereby allowing the material to yield at greatly reduced stresses. There is also a growing body of evidence to show that rubber particle cavitation is a necessary precursor to multiple crazing in toughened glassy polymers such as ABS and HIPS (high-impact polystyrene).[33,34]

The strong concentration of damage in bands emanating from the crack tip indicates an unstable material behavior against damage and deformation. This inhomogeneous damage distribution may be considered as suboptimal. Smit[35] demonstrated that material deformation instability is related to strain softening and has an adverse effect on toughness. If cavitation of the rubber particles is achieved in regions of high tensile stress, the polymer can deform plastically by shear yielding before craze initiation takes place. Ideally, this plastic flow process is activated in the entire matrix, thus resulting in massive energy dissipation and hence increase of fracture toughness. Indeed, ABS shows strain softening, and the present investigation illustrates that material instability results in severely localized damage. However, this study also demonstrates that ABS allows an extreme amount of damage before actual material separation occurs. Further improvement of the toughness of ABS might be achieved by reducing the unstable deformation and damage behavior.

MRI images of PBT/PTMO differ significantly from those of ABS. Figure 6a shows an image of PBT/PTMO under critical load (around 29% elongation). The stress−strain relation obtained in the straining device is presented in Figure 7. The PBT/PTMO block copolymer

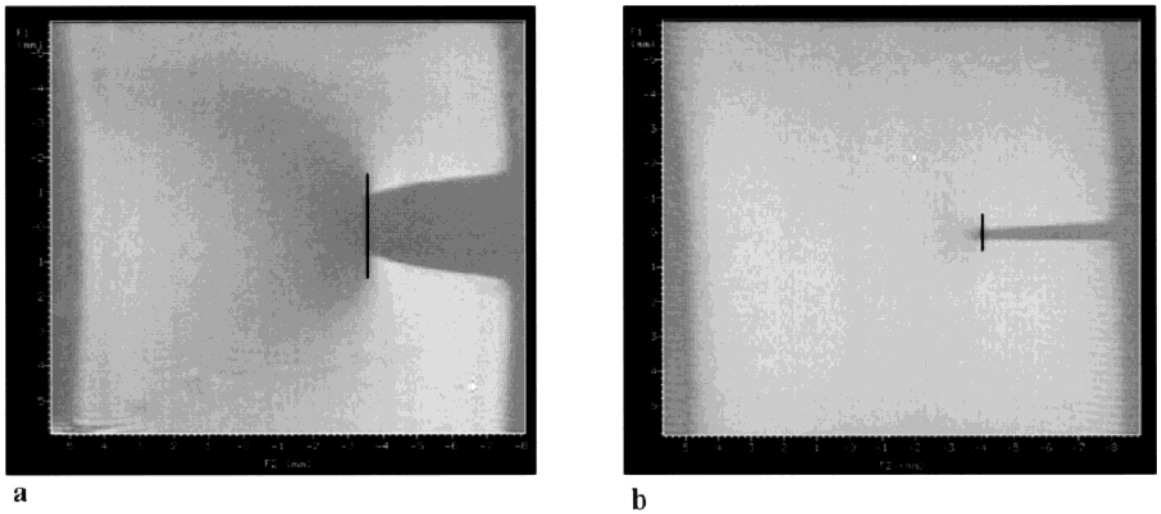

Figure 6. (a) Slice selective image of PBT/PTMO under critical load; (b) idem after unloading. The depth of the original notch is indicated by a vertical line.

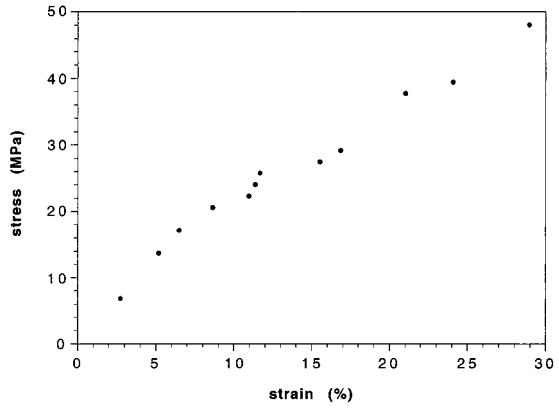

Figure 7. Stress−strain curve measured for PBT/PTMO.

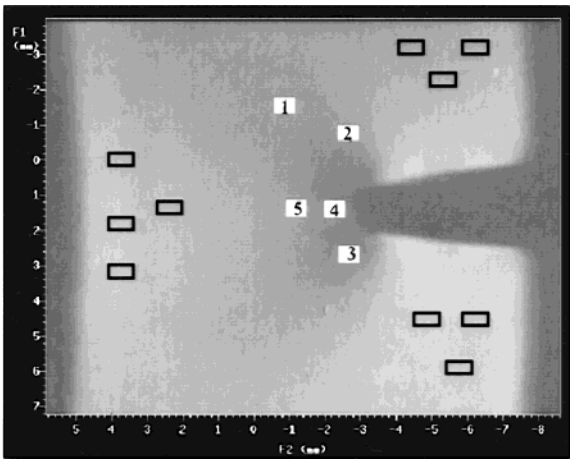

Figure 8. Image of PBT/PTMO showing the fixed spatial locations where the quantitative spin density (M_0) and T_1 and T_2 relaxation times were determined. For values see Table 2. The reference spots (black rectangles) are located at least 1.5 mm from the damage bands.

is much more ductile. Strain induced response in the proximity of the crack tip for PBT/PTMO differs strongly from this in ABS, as can be observed by comparing Figures 3 and 6a. The PBT/PTMO block copolymer reveals a more continuous distribution of stress induced material response, emanating from the tip of the notch.

Table 2 shows the quantitative, spatial dependent results of M_0, T_2, and T_1 for the block copolymer. Upon loading, a reduction of the plate thickness due to Poisson contraction (ca. 0.5 mm visible by eye) occurs around the crack tip. Therefore, plate centered, slice selective images (thickness of 2 mm) were acquired to exclude the reduction of the plate thickness around the crack tip from the quantitative data. In contrast to ABS, a significant spatial dependency, compared to unaffected reference locations, can be observed for T_2 around the crack tip. The decrease in T_2 can be ascribed to a decrease in long-range mobility of PTMO chains due to strain induced chain alignment, since PBT/PTMO block copolymers with short PTMO blocks show strain induced chain orientation but no crystallization.[36] This is confirmed by a previous ^{13}C NMR study of Schmidt et al.[28] Unstrained PBT/PTMO block copolymers with a large block length (1500−2000 g/mol) and high amount of PTMO (60 wt %) show a clear phase separation into mobile PTMO-rich domains and more rigid mixed PTMO/PBT domains. Uniaxial stretching of these block copolymers results in a strain induced crystallization in the mobile PTMO-rich domains. The crystallinity increases with increasing PTMO content and the block length. Noncrystalline PTMO chains become oriented but less than the crystalline.

Table 2. Spatial Dependence of the Spin Density (M_0) and T_2 and T_1 Relaxation Time for PBT/PTMO under Critical Load; the Positions Are Indicated in Figure 8[a]

	loaded			
fixed spatial position	T_2 (ms)	M_0	T_1 (s)	M_0
1	0.41	100	0.80	96
2	0.40	52	0.81	53
3	0.40	74	0.79	70
4	0.43	47	0.83	51
5	0.42	100	0.83	100
ref	0.56	100	0.84	100

[a] The averaged 95% confidence limit is 3% for the relaxation times and 2% for the M_0 values.

A decrease in the spin density (M_0) is only observed close to the crack tip (Table 2; see locations 2−4). Since cavitation in PBT/PTMO is expected to be low, the decrease in M_0 under load possibly is caused by a significant decrease in segmental mobility of some of the PTMO chains. Figure 6b shows that unloading of the PBT/PTMO block copolymer results in an almost complete vanishing of strain induced chain orientation (T_2 effect) and spin density effect.

Conclusions

It has been demonstrated that spin-warp NMR imaging, which detects only soft phases in polymer materials, is a useful method to study the crack growth resistance of polymers. Under conditions of critical load, damage bands appear in the images of ABS while the PBT/PTMO block copolymer reveals a more continuous stress distribution in the proximity of the crack tip. Valuable, complementary information is provided by the spatial resolved values of the spin density and the T_2 and T_1 relaxation times. This quantification of image contrast is of particular interest for a better understanding of the process of fracture of polymer materials. The images clearly indicate that damage bands in ABS mainly arise from a large decrease in material density which is caused by severe rubber particle cavitation. No significant strain induced orientation of the rubbery chains in ABS is observed. In the case of the PBT/PTMO block copolymer, a significant orientation of the PTMO chains is observed in the proximity of the crack tip. While the damage bands in ABS remain present upon unloading, chain alignment in PBT/PTMO block copolymers with rather short block length and small amount of PTMO largely disappears upon unloading.

Acknowledgment. The authors are thankful to the European Community ("Europees Fonds voor Regionale Ontwikkeling") and Limburgfonds (GOM Limburg) for the financial support, J. Kaelen for the technical support in constructing the stretching device, and Ir. L. Naelaerts for the tensile strength tests.

References and Notes

(1) Sha, Y.; Hui, C. Y.; Ruina, A.; Kramer, E. J. *Macromelecules* **1995**, *28*, 2450.
(2) Brown, H. R. *Macromolecules* **1991**, *24*, 2752.
(3) Donald, A. M.; Kramer, E. J. *Philos. Mag. A* **1981**, *43* (4), 857.
(4) Döll, W. *Adv. Polym. Sci.* **1983**, *52* (3), 105.
(5) Brown, H. R.; Ward, I. M. *Polymer* **1973**, *14*, 468.
(6) Marissen, R. *Polymer* **2000**, *41*, 1119.
(7) Shoolenberg, G. E. A Study of the Ultra-Violet Degradation Embrittlement of Polypropylene Polymer. Ph.D. Thesis, Delft University of Technology, 1988.
(8) Bucknall, C. B.; Heather, P. S.; Lazzeri, A. *J. Mater. Sci.* **1989**, *16*, 2255.
(9) Dijkstra, K. Deformation and Fracture of Nylon-6-Rubber Blends. Ph.D. Thesis, Twente University of Technology, ISBN 90-9005816-8, Feb 1993.
(10) Dijkstra, K.; Laak, J.; Gaymans, R. J. *Polymer* **1994**, *35*, 315.
(11) Lu, X.; Brown, N. *J. Mater. Sci.* **1991**, *26*, 612.
(12) Muratoglu, O. K.; Argon, A. S.; Cohen, R. E.; Weinberg, M. *Polymer* **1995**, *36* (25), 4771.
(13) Riemslag, T. Crack Growth in Polyethylene. Ph.D. Thesis, Delft University of Technology, June 1997.
(14) Riemslag, A. C. *J. Test. Eval.* **1994**, *22*, 410.
(15) Blümich, B., Kuhn, W., Eds. *Magnetic Resonance Microscopy: Methods and Applications in Materials Science, Agriculture and Biomedicine*; VCH Publishers: New York, 1992.
(16) Callaghan, P. T. *Principles of Nuclear Magnetic Resonance Microscopy*; Clarendar Press: Oxford, 1991.
(17) Weigand, F.; Spiess, W. H. *Macromolecules* **1995**, *28*, 6361.
(18) Blümler, P.; Blümich, B. *Acta Polym.* **1993**, *44*, 125.
(19) Traub, B.; Hafner, S.; Wiesner, U.; Spiess, H. W. *Macromolecules* **1998**, *31*, 8585.
(20) Günther, E.; Blümich, B.; Spiess, H. W. *Macromolecules* **1992**, *25*, 3315.
(21) Hepp, M. A.; Miller, J. B. *J. Magn. Reson. A* **1994**, *111*, 62.
(22) Klinkenberg, M.; Blümler, P.; Blümich, B. *J. Magn. Reson. A* **1996**, *119*, 197.
(23) Klinkenberg, M.; Blümler, P.; Blümich, B. *Macromolecules* **1997**, *30*, 1038.
(24) Hauck, D.; Blümler, P.; Blümich, B. *Macromol. Chem. Phys.* **1997**, *198*, 2729.
(25) Kuhn, W. *Angew. Chem., Int. Ed. Engl.* **1990**, *29*, 1.
(26) Adriaensens, P.; Pollaris, A.; Vanderzande, D.; Gelan, J.; White, J. L.; Dias, A. J.; Kelchtermans, M. *Macromolecules* **1999**, *32*, 4692.
(27) Ercken, M.; Adriaensens, P.; Vanderzande, D.; Gelan, J. *Macromolecules* **1995**, *28*, 8541.
(28) Schmidt, A.; Veeman, W. S.; Litvinov, V. M.; Gabriëlse, W. *Macromolecules* **1998**, *31*, 1652.
(29) Liu, J.; Nieminen, A. O. K.; Koenig, J. L. *J. Magn. Reson.* **1989**, *85*, 95.
(30) Weigand, F.; Hafner, S.; Spiess, H. W. *J. Magn. Reson.* **1996**, *120*, 201.
(31) Bucknall, C. B. In *The Physics of Glassy Polymers*, 2nd ed.; Haward, R. N., Young, R. J., Eds.; Chapman & Hall: London, 1997.
(32) Bucknall, C. B. In *Polymer Blends: Formulation and Performance;* Paul, D. R., Bucknall, C. B., Eds.; Wiley: New York, 1999; Chapter 22.
(33) Giaconi, G. F.; Castellani, L.; Maestrini, C.; Riccò, T. *Polymer* **1998**, *39* (25), 6315.
(34) Bucknall, C. B.; Rizzieri, R.; Moore, D. R. Detection of incipient rubber particle cavitation in toughened PMMA using dynamic mechanical tests. *Polymer*, in press.
(35) Smit, R. J. M. Toughness of heterogeneous polymeric systems, a modeling approach. Ph.D. Thesis, Eindhoven University of Technology, June 1998.
(36) Soliman, M., private communication.

MA991675T